

# Resonant Engines

An E1P-Derived Biased-Parametric Electromagnetic Machine

Resonant Institute

## Abstract

This working paper organizes a rigorous research program for developing a new rotary electromagnetic machine, termed here a **resonant engine**. The candidate machine combines a permanent-magnet-biased rotor, two superposed stator winding sets that realize distinct magnetic-circuit roles, and a resonant converter/control stack intended to alternate between those roles near half the mechanical rotation frequency. E1P is used here as a design-generating framework: it supplies the architecture logic and the measurement hypotheses, but the standard of progress is experimental clarity and engineering usefulness rather than theoretical defense.

Accordingly, the paper has five practical aims: to define the candidate architecture precisely enough for modeling and prototyping; to state the main engineering hypotheses that make the concept worth building; to distinguish the engine's **architectural identity** from the **control regimes** used to extract useful performance; to specify the measurements required to separate intended behavior from ordinary commutation artifacts; and to lay out a development program with clear decision gates. The central research questions are whether alternating  $\alpha/\beta$  stator states produce behavior not reducible to conventional two-phase operation, whether a preferred operating regime appears near  $\omega_{\text{swap}} = \omega_{\text{mech}}/2$ , whether the predicted spectral signature can be preserved under practical motoring control, and whether cross-scale coherence materially affects load response, thermal derating, and duty-cycle efficiency.

Stage 1 of the digital twin — a symbolic-analytical model — established the canonical three-line signature as a closed-form consequence of the tetrad cycle under idealized drive, with numerical FFT confirming analytical amplitudes to machine precision. An early Stage 2 validation pass reproduced that canonical result exactly under idealized conditions, but also showed that the canonical half-order current family behaves as a **native resonant signature baseline rather than a complete motoring controller**: it yields the expected spectral structure while producing near-zero mean torque. This finding does not invalidate the architecture. Instead, it motivates a dual-regime development path: a **native resonant regime**, where the architecture is studied in its most distinct E1P-derived form, and a **hybrid motoring regime**, where a rotor-synchronous torque-producing carrier is added so that the same architecture can be evaluated as a practical engine. These are not mutually exclusive time-sliced modes. In the intended efficient-engine pathway, the hybrid motoring regime is implemented by **superposing** the motoring carrier on the native resonant  $\alpha/\beta$  alternation, so that both functions are active at the same time: one layer supplies mean shaft torque, and the other preserves the resonant signature and its associated envelope-performance and diagnostic advantages.

The paper does not report prototype data, completed finite-element optimization, or a final novelty determination. Energy conservation, charge continuity, and magnetic-flux closure remain

hard constraints throughout. The contribution claimed here is a disciplined research framework for developing and testing one. The paper’s scope is deliberately machine-scale; the broader architectural-family context in which the resonant engine sits — including its relation to other frameworks that treat the tetrad cycle as substrate-independent, and the cosmic-scale instances of the same architecture — is developed in the companion papers *Solar Systems as Resonant Engines*, and *Resonant Engines as Localised Solar Systems* (Resonant Institute, 2026) and *DNA as a Resonant Engine* (Resonant Institute, 2026). The three papers are intended to be read together.

## 1. Introduction

### 1.1 Research aim

This document is written to advance rigorous research on a new type of electromagnetic engine, not to defend a closed theoretical position. Its value is practical: it should help decide what to build, what to measure, what to compare against, and what evidence would justify continuing, revising, or abandoning a given branch of the concept.

E1P matters in this paper only to the extent that it generates useful engineering consequences. The relevant question is not whether the framework can be restated elegantly, but whether it improves development by yielding architecture choices, observables, and experimental constraints that would otherwise be easy to miss.

### 1.2 Scope of this paper

This is a working research paper. We do not claim validated performance, completed optimization, patent-grade novelty clearance, or settled proof of every interpretive step. The paper does four narrower things:

1. define the candidate machine architecture currently under investigation;
2. state the engineering hypotheses that make the concept worth prototyping;
3. specify the measurements and comparison baselines needed for rigorous evaluation; and
4. organize the next development stages into concrete work packages and decision gates.

### 1.3 What this draft is meant to deliver

The paper is intended to function as a shared technical reference for the research program. Its main outputs are:

1. an architecture description precise enough for first modeling and prototyping;
2. a minimal set of observables: torque/speed, current/voltage, temperature, and spectral content around  $\omega_{\text{mech}}$  and  $\omega_{\text{mech}}/2$ ;
3. a prototype test matrix that distinguishes intended behavior from ordinary commutation artifacts;
4. a map of related machine families that helps define meaningful baselines; and
5. a list of unresolved engineering decisions in order of constraint propagation.

### 1.4 Standard of progress

Progress in this program should be judged by disciplined iteration:

model  $\rightarrow$  build  $\rightarrow$  instrument  $\rightarrow$  measure  $\rightarrow$  decide.

A good research document in this setting does not overstate novelty or certainty; it makes uncertainty operational. Each claim below is therefore framed as a working architectural choice, engineering hypothesis, measurement proposal, or development priority.

## 2. E1P assumptions used operationally in this program

We assume familiarity with the E1P Primer and the associated electromagnetism manuscript. Only the elements that directly influence design choices are retained here, and they are used operationally: as inputs to architecture and testing, not as standalone objects of defense.

### 2.1 Core relation and phase structure

E1P begins from the zeroth-law relation

$$E \equiv A/C \rightleftharpoons 1$$

where energy is expressed as the ratio of Active to Connective components resonant to unity. The tetrad  $\{AA, CC, CA, AC\}$  cycles as

$$AA \rightarrow CC \rightarrow CA \rightarrow AC \rightarrow AA^+,$$

with  $AA^+$  denoting an activated continuation rather than a simple return to the initial state. For the present research program, the important engineering consequence is that a geometrically repeated state may still play a different role in the cycle. That is what motivates looking for two-turn behavior instead of assuming that one mechanical revolution must exhaust the machine's meaningful dynamics.

### 2.2 Electromagnetic identification

The specific E1P identification used here is

- **Active = Electric**
- **Connective = Magnetic**

This is a structural correspondence established in the companion electromagnetism manuscript: every defining character of Active maps to electric phenomena, and every defining character of Connective maps to magnetic phenomena, without remainder. In that reading, the magnetic constraint  $\nabla \cdot \mathbf{B} = 0$  is not just an observed regularity; it is the statement that magnetic connectivity must always close. For readers who do not adopt the full E1P framing, the operational implication still holds: magnetic closure deserves to be treated as a first-class architectural constraint.

### 2.3 Design consequence: magnetic closure as an engineering objective

Once closure is treated as a design driver, the relevant question for any machine becomes: *where does the magnetic field close, and how much of that closure path contributes to useful work?*

Any portion of the closure path spent in back-iron, leakage space, or geometrically non-working substrate becomes an explicit target for design improvement. In E1P language this is remainder; in standard engineering language it is non-productive magnetic expenditure.

## **2.4 Alternation as a development hypothesis**

A second E1P premise used programmatically here is that fulfilment of one pole generates the gradient toward its complement. Mapped into electromechanical design, that suggests exploring a machine in which alternation between two magnetic-circuit states is not merely tolerated by the controller but deliberately exploited. Whether that produces a useful engine is a research question, not a settled result. The value of the premise is that it points toward a specific class of architecture worth testing.

## **3. Working design logic**

The argument in this section should be read as design logic for the current research branch. Its purpose is to explain why the candidate architecture looks the way it does and what experimental consequences follow from those choices.

### **3.1 Closure-oriented topology selection**

Conventional radial-flux PMSMs close magnetic flux through teeth, back-iron, and return path. Some of that flux performs useful air-gap work; some of it closes through mechanically necessary but electromagnetically non-productive structure. Axial-flux layouts can shorten closure paths, and Halbach arrays can bias field concentration toward the working face while suppressing it on the opposite face.

From the present viewpoint, Halbach-style field shaping is noteworthy because it attempts to place magnetic closure where the designer wants the machine to work. Pushed further, that logic points toward ironless or near-ironless arrangements in which the working gap is a major part of the closure path instead of a small interruption in a larger magnetic return structure. That does not uniquely determine the final machine geometry, but it does constrain the family of geometries worth prioritizing in research.

### **3.2 Rotor as standing magnetic bias substrate**

Permanent magnets provide a standing magnetic bias. In the present architecture they are assigned a stabilizing role: the rotor provides the magnetic substrate against which the stator executes the alternating cycle. This is a different functional emphasis from a conventional PMSM, where the rotor magnets are primarily discussed through their role in torque production against a rotating stator field.

For the research program, the practical implication is that rotor design should prioritize bias stability, thermal robustness, and invariance across the intended operating sequence. The rotor does not need to reconfigure every turn; it needs to present a repeatable magnetic boundary condition to whichever stator topology is active.

### **3.3 Two working states**

The current concept explores two complementary stator states:



- **Connective-biased state.** The stator-rotor circuit is biased toward maximal stored magnetic field.
- **Active-biased state.** The same hardware is biased toward maximal work delivery and transit of energy through torque production.

These labels should be treated as design intent, not as claims that one state contains “all” the energy and the other none. The research question is whether two deliberately distinct magnetic-circuit roles can be implemented cleanly enough that alternating between them produces measurable benefits or signatures beyond ordinary two-phase commutation.

### 3.4 Working hypothesis: why the proposal may imply a 720° cycle

A 360° rotor rotation restores the rotor to the same geometric orientation. Within the present E1P reading, that need not imply return to the same energetic role in the cycle. The distinction between  $AA$  and  $AA^+$  is precisely that a configuration may repeat geometrically while differing in cycle function. If that distinction has engineering consequences, one full mechanical revolution is not enough to complete the relevant operating sequence.

This leads to a two-turn working hypothesis: one turn in which the Connective-biased state is the fulfilled state and the Active-biased state supplies the gradient, followed by a complementary turn in which those energetic roles are reversed. The important point for development is not the language itself but the measurement consequence: a meaningful two-turn interpretation should leave observable traces, especially around half-order spectral content, conjugate-pair structure, and turn-to-turn state dependence.

This remains a hypothesis. A prototype that shows no measurable distinction between the first and second revolutions would weaken or eliminate the need for the 720° framing.

### 3.5 Why alternation is placed in the stator

There are, in principle, three places to locate the role-swap: in the rotor, in the stator, or in a distributed mechanism spanning both. The present research branch places it in the stator for three reasons.

**Structural consistency.** If the rotor supplies the standing magnetic bias and the electrical drive enters through the stator, placing the alternation in the stator keeps the active cycling in the electrically active subsystem.

**Engineering practicality.** Stationary windings are easier to cool, instrument, insulate, and switch than rotating electrical structures. Moving reconfiguration into the rotor would add slip interfaces, switched rotating elements, or mechanically modulated structures that are harder to package and diagnose.

**Control economy.** The resonant converter already interfaces with the stator. If the same converter both performs impedance matching and executes the  $\alpha/\beta$  alternation, the architecture remains compact: one subsystem provides both excitation and state management.

### 3.6 Integration-centered design principles

The design logic should now be stated more explicitly. The resonant engine should not be optimized around symmetry alone, nor around alternation as an end in itself. It should be optimized around the creation and maintenance of a **productive interaction zone** — a CA-like

integrating field node — in which differentiated magnetic-circuit states are held in coherent tension and converted into useful work.

This leads to five design principles.

**First: design around an integrating field node, not just two opposed states.** The point of creating distinct  $\alpha$  and  $\beta$  topologies is not merely to demonstrate alternation. It is to create a stable interaction zone in which those opposed states remain legible, coupled, and capable of productive transfer. The working gap and active torque-production region should therefore be treated as the machine’s integrating heart, not as a passive space between source and return structures.

**Second: preserve explicit phase roles in the hardware.** The architecture is strongest when AA, CC, CA, and AC are not merely interpretive labels but design functions. The rotor bias and reference geometry supply the AA role; the retained magnetic-storage condition supplies the CC role; the active interaction zone where useful transfer occurs supplies the CA role; and the detuning, pruning, and recovery boundary conditions in control and converter timing supply the AC role. The machine should therefore be designed as a four-role architecture, even when those roles are physically coupled.

**Third: the subsystem that creates differentiation should also be capable of restoring integration.** In mature operation, the element that establishes the distinction between  $\alpha$  and  $\beta$  should also help hold them in productive relation under load. This makes the converter-control layer more than a power supply: it becomes the governor of the integrating state, responsible both for creating contrast and for re-establishing coherent relation when detuning, load, or temperature disturb it.

**Fourth: design out failed thresholds.** Any region in which field energy accumulates but fails to become useful torque should be treated as a structural defect rather than an acceptable by-product. In practice, this means locating and reducing torque dead zones, non-productive closure paths, impulsive handoff intervals, and converter states that generate signature without useful work. A strong resonant engine should minimize these failed-threshold regions rather than merely diagnosing them after the fact.

**Fifth: prefer shared-field control over purely pairwise commutation logic.** The machine’s control problem should not be treated only as a sequence of bilateral switching events between separate elements. It should also be treated as the regulation of a single coherence state spanning rotor bias,  $\alpha/\beta$  relation, converter timing, spectral symmetry, and thermal drift. The most useful controller is therefore the one that estimates and maintains this shared state directly.

### 3.7 One architecture, two operating regimes

The present paper now distinguishes clearly between the **architecture** of the resonant engine and the **control regimes** used to operate it.

The architecture is singular: PM-biased rotor, dual superposed stator windings, an explicitly engineered interaction zone in which their opposition becomes productive transfer, and a converter-control layer capable of controlled  $\alpha/\beta$  alternation and coherence maintenance. That architecture can then be studied under two operating regimes. The critical clarification is that these regimes are conceptually distinct but physically compatible: they can be investigated

separately for clarity, but in the intended practical engine they are expected to be **co-present layers of the same operating state**, not two unrelated modes that must be chosen between.

**Native resonant regime.** In this regime, the half-order  $\alpha/\beta$  alternation is primary. This is the cleanest regime for asking whether the architecture is genuinely distinct, whether the  $720^\circ$  / half-order interpretation leaves measurable traces, and whether the predicted spectral signature survives experimental scrutiny. It is the regime that best preserves the original v0.4 proposition.

**Hybrid motoring regime.** In this regime, a rotor-synchronous torque-producing carrier is added while the resonant  $\alpha/\beta$  alternation remains present as a modulation layer. This is the practical engineering regime in which the machine is judged on positive mean torque, efficiency maps, low-speed operation, thermal derating behavior, and matched baseline comparisons. It should therefore be understood not as a replacement for the native resonant regime, but as the case in which the native resonant layer and the motoring layer are used **at the same time**.

The development program should not force a premature choice between these regimes. The native resonant regime protects the engine’s architectural distinctiveness; the hybrid motoring regime tests whether that same architecture can become a commercially useful engine. Failure of the native regime to provide competitive mean torque would not by itself invalidate the architecture if the hybrid regime preserves the resonant signature and the envelope advantages that motivate the concept.

### 3.7 Topology plates and the canonical E1P cross schema

Figures 1–4 make the present design logic visible across a small family of machine realizations. Two are intentionally classical reference points — a PMDC-like implementation and an electronically commutated PMSM-like implementation — and two extend the same architectural logic into geometries that are more native to the closure-oriented program: a shape-optimised axial-flux topology and a field-following lobed geometry. Taken together, the four plates are not offered as finished production drawings. They are working architectural figures that show how the same tetrad-closure requirement can be instantiated across more than one motor family.

A terminology and presentation point should also be fixed here. The only official E1P cycle schematic used in this paper is the **canonical cross schema**:  $AA$  at left,  $CC$  at right,  $CA$  at top, and  $AC$  at bottom. Earlier square-cycle or loop-cycle renderings are not used here as the canonical figure form. The topology plates below have therefore been standardised around the cross-schema presentation.

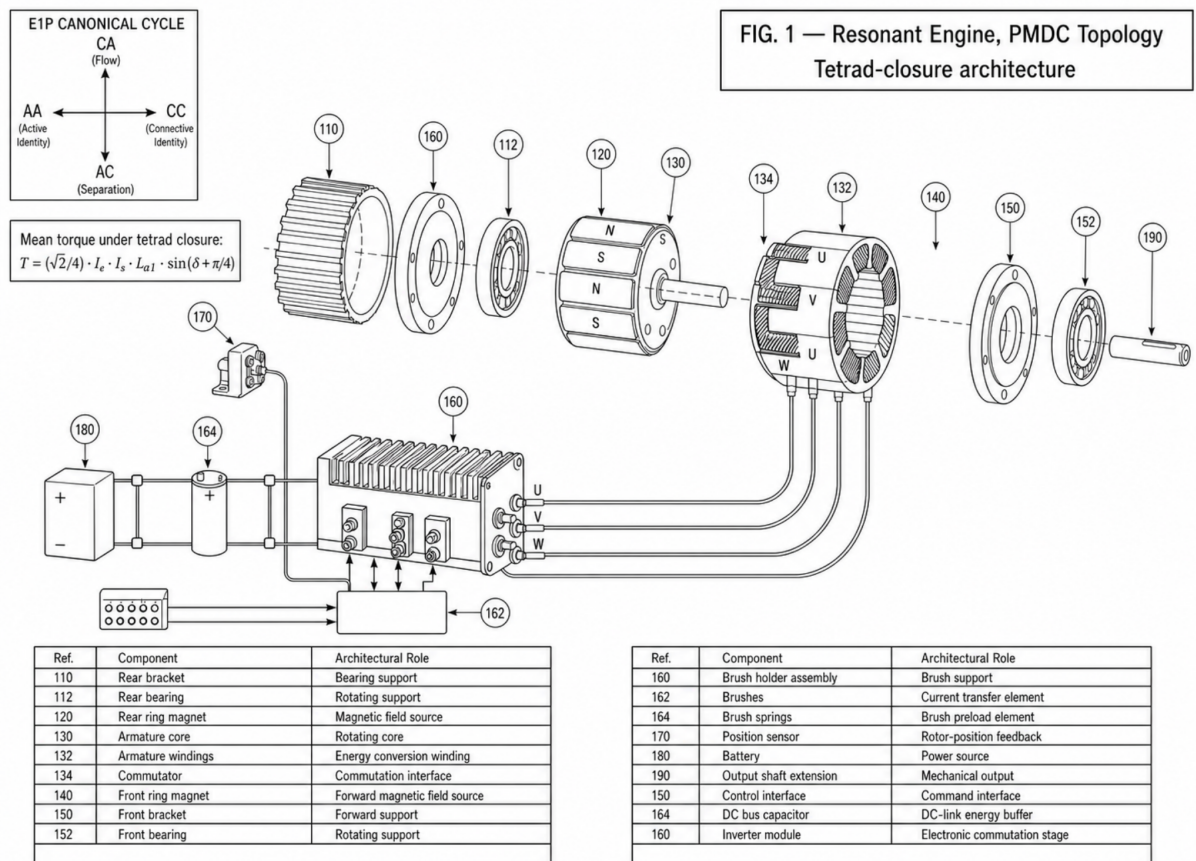


Figure 1: PMDC-style resonant-engine topology plate. The image itself carries the full component callouts and architectural-role mapping.

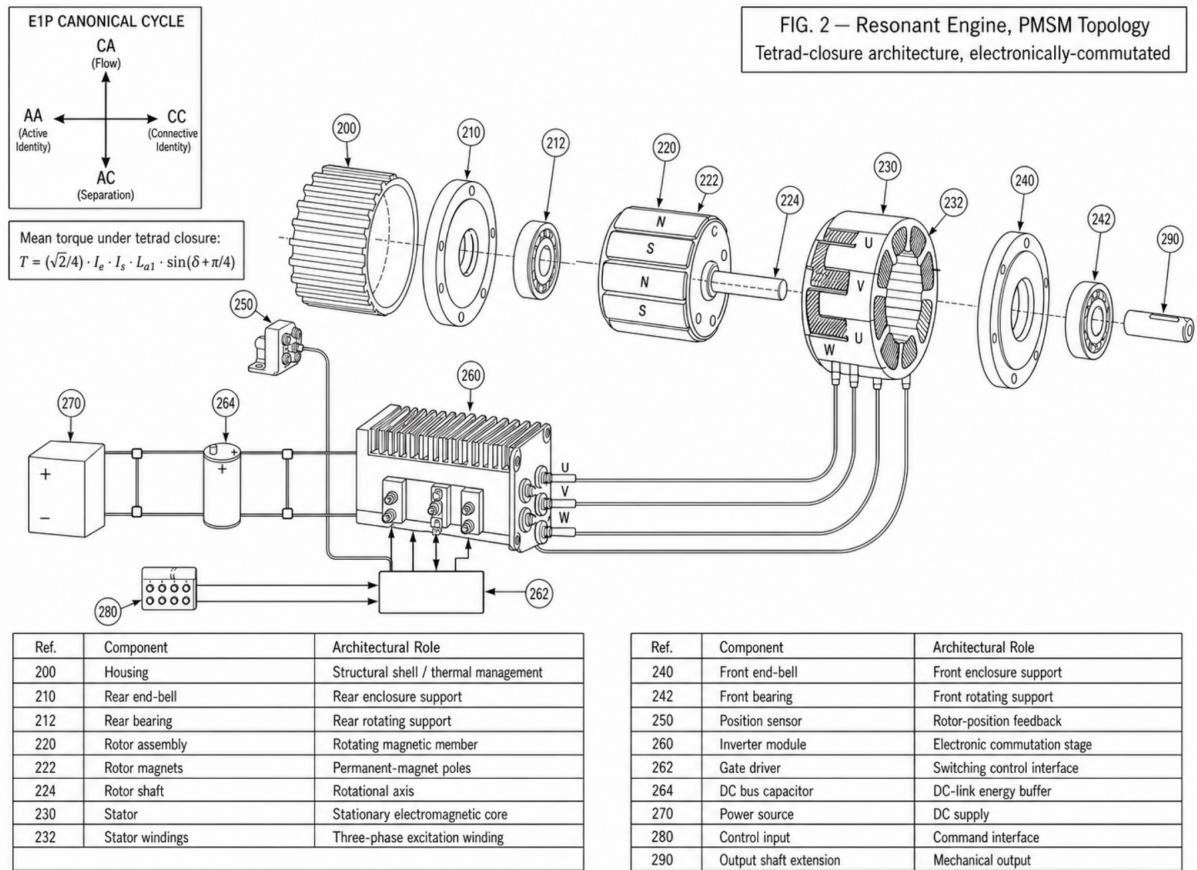


Figure 2: PMSM-style resonant-engine topology plate. This figure shows the electronically commutated reference implementation of the same tetrad-closure architecture.

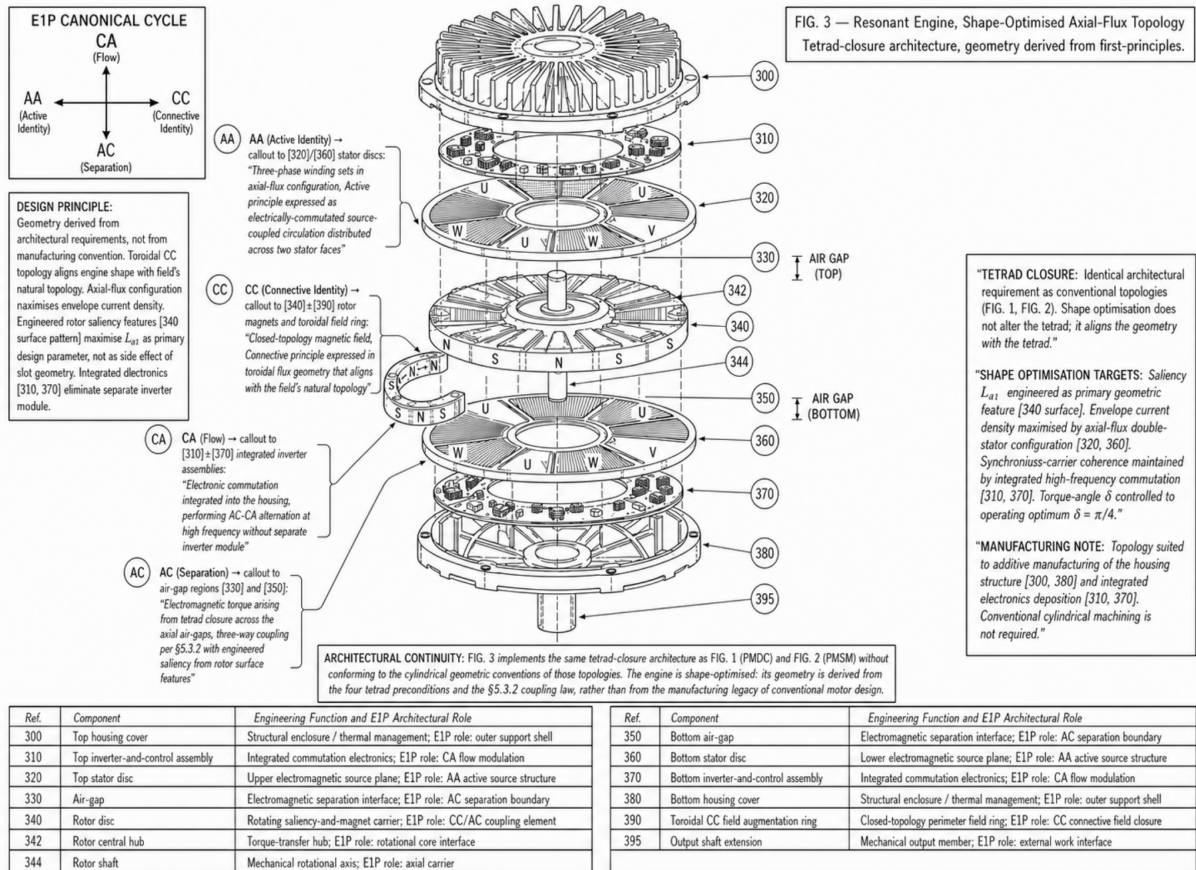


Figure 3: Shape-optimised axial-flux resonant-engine topology plate. The figure illustrates a geometry derived from the paper's closure-oriented design logic rather than from cylindrical motor legacy.



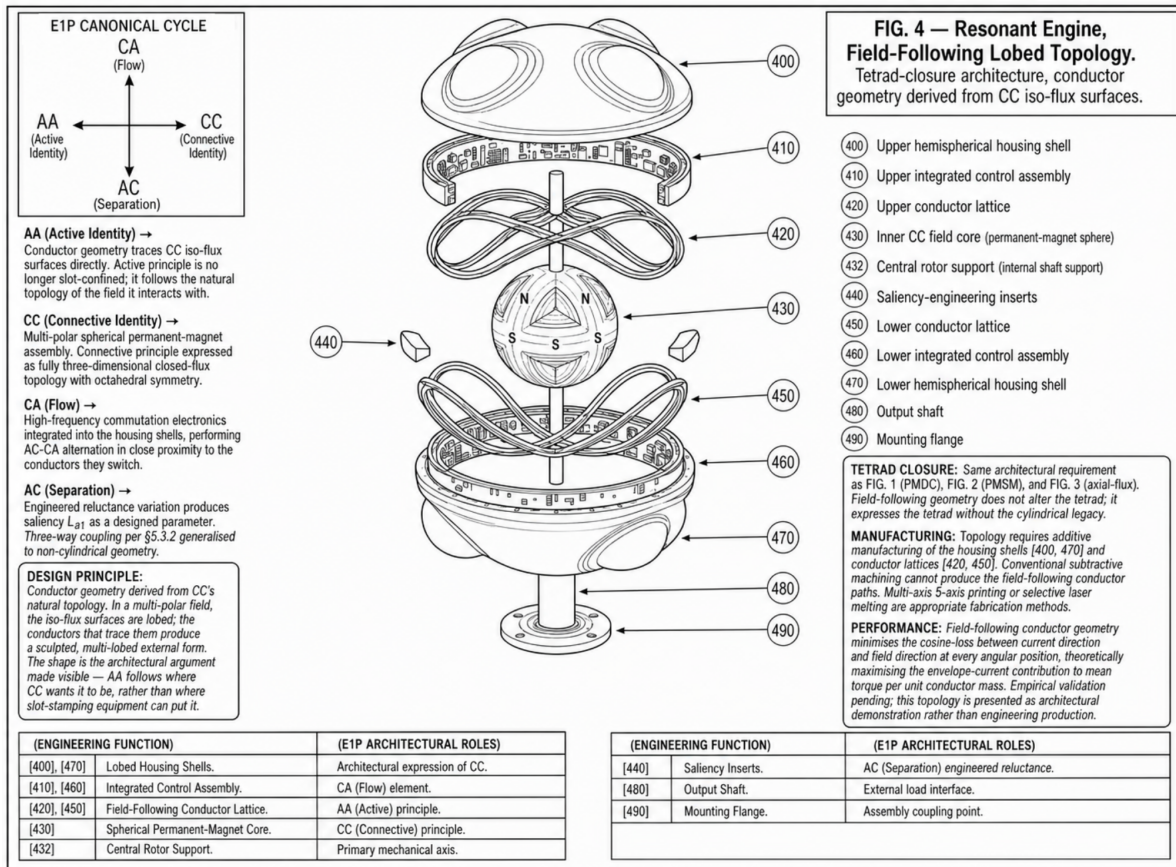


Figure 4: Field-following lobed resonant-engine topology plate. This figure presents the most geometry-liberated topology in the current family.

## 4. Candidate research architecture

### 4.1 System overview

The candidate resonant engine currently under study consists of five coupled subsystems:

1. **Rotor reference.** A permanent-magnet-biased rotor with a single intended magnetic bias state and  $360^\circ$  geometric periodicity. Its primary function is to supply a stable reference and standing magnetic substrate rather than to carry the full burden of dynamic reconfiguration.
2. **Differentiated stator pair.** Two superposed winding sets, denoted  $\alpha$  and  $\beta$ , arranged so that each realizes a distinct magnetic-circuit topology through the same rotor. These should be treated as deliberately differentiated populations, not merely as ordinary commutation phases.
3. **Active interaction zone.** The working air gap and associated flux-transfer region in which the opposition between  $\alpha$  and  $\beta$  is converted into useful transfer. This zone should be designed as the machine's integrating field node rather than as passive empty space.
4. **Converter-control governor.** A resonant power stage and control layer that alternates excitation between  $\alpha$  and  $\beta$  at  $\omega_{\text{swap}}$ , superposes motoring current where needed, and maintains the shared coherence state of the machine under load, detuning, and thermal drift.
5. **Instrumentation layer.** Electrical and mechanical sensing intended to detect half-order content, switching residuals, torque production, thermal drift, and loss of coherence under load.

This system overview should be read functionally. The engine is not only a rotor, stator, and converter; it is a source-reference, a differentiated pair, an integrating interaction zone, and a governor that must keep that interaction productive.

### 4.2 Rotor specification (preliminary)

- **Bias magnet grade.**  $\text{Sm}_2\text{Co}_{17}$  (e.g., Recoma 35E class) is the preferred provisional candidate because thermal stability of the standing magnetic bias is load-bearing for the cross-scale coherence hypothesis (§5.4). The reversible temperature coefficient of remanence  $\alpha(B_r)$  for  $\text{Sm}_2\text{Co}_{17}$  is approximately  $-0.035\%/^\circ\text{C}$ , versus approximately  $-0.12\%/^\circ\text{C}$  for NdFeB grades including N52 and N42SH [Arnold Magnetic Technologies datasheets]. Over a  $100^\circ\text{C}$  operating swing, NdFeB loses approximately 12% of  $B_r$  reversibly while  $\text{Sm}_2\text{Co}_{17}$  loses approximately 3%. For a resonant architecture whose stored field energy scales as  $B_r^2$ , this corresponds to approximately 24% versus 6% drift in the standing-bias substrate.  $\text{Sm}_2\text{Co}_{17}$  also exhibits a substantially higher Curie temperature ( $\sim 820^\circ\text{C}$  vs  $\sim 310^\circ\text{C}$  for NdFeB) and a higher maximum operating temperature ( $\sim 300^\circ\text{C}$  vs  $\sim 80\text{--}150^\circ\text{C}$  depending on grade) [Gutfleisch et al., 2011]. Final selection should be made only after a coupled thermal-magnetic sensitivity study, but the quantitative case for SmCo on the thermal-coherence axis is straightforward from verified vendor data.
- **Magnetization pattern.** Still open. Surface-mounted, interior, and rotor-internal Halbach arrangements remain candidates. The governing question is which pattern presents the cleanest repeatable magnetic boundary condition to both  $\alpha$  and  $\beta$ .
- **Geometric symmetry.** The rotor should be  $360^\circ$  periodic. Any two-turn behavior that matters to the concept should therefore arise from the stator-plus-converter sequence, not from a geometrically asymmetric rotor.



### 4.3 Stator specification (preliminary)

- **Two superposed winding sets.**  $\alpha$  and  $\beta$  should each be capable of completing a magnetic circuit through the rotor, but they should not collapse into the same effective topology. Their purpose is to create legible differentiated states whose opposition can later be held in productive relation.
- **Topology  $\alpha$ .** Intended to favor the stored-field or Connective-biased condition.
- **Topology  $\beta$ .** Intended to favor the work-delivery or Active-biased condition.
- **Active interaction region.** The geometry should be judged not only by what each topology does separately, but by how the pair creates a coherent working region between them. This region is where useful torque, spectral identity, and phase-sensitive transfer should all become most legible.
- **Geometric relation between  $\alpha$  and  $\beta$ .** Still open. The sets must be distinct enough to preserve a meaningful two-state alternation, yet sufficiently overlapping that the transition between states does not create an excessive torque dead zone or purely impulsive handover. Any geometry that generates persistent non-productive handoff intervals should be treated as containing a failed threshold that must be redesigned out.
- **Nearest hardware families.** The closest hardware families remain dual-wound synchronous machines, flux-switching machines, PM-biased reluctance layouts, and stepper-adjacent topologies. These define comparison baselines rather than a final geometry choice.

### 4.4 Converter and control specification (preliminary)

- **Converter family.** Candidate families include series-resonant, LLC, and dual-active-bridge variants. Selection depends on the realized inductance profile of the machine, which in turn depends on stator geometry.
- **Two control regimes, one machine.** The present research branch no longer treats the control question as all-or-nothing. The same hardware must support two explicit operating regimes. These regimes must be separable in analysis, but compatible in implementation.
  1. **Native resonant mode**, in which the half-order  $\alpha/\beta$  alternation is the primary actuation and diagnostic structure.
  2. **Hybrid motoring mode**, in which a rotor-synchronous torque carrier is superposed on the  $\alpha/\beta$  alternation so that the machine can deliver positive mean shaft torque while preserving a measurable resonant signature.
- **Simultaneity requirement.** For the efficient-engine pathway, the practical target is not time-sharing between a resonant mode and a motoring mode. The practical target is a **composite operating state** in which the resonant  $\alpha/\beta$  layer and the torque-producing synchronous layer are active concurrently. The motoring layer supplies useful average shaft work; the resonant layer preserves the designed spectral signature and the associated diagnostic, detuning, and envelope-performance behavior.
- **Alternation frequency.** The working hypothesis still predicts a preferred region near

$$\omega_{\text{swap}} = \omega_{\text{mech}}/2.$$

In v0.11 this relation is interpreted as the preferred tuning rule for the resonant regime and the resonant layer of the hybrid regime. It is not assumed in advance that the half-order envelope alone must carry the full burden of motoring.

- **Phase advance and synchronous alignment.** The hybrid motoring mode requires a

controllable phase-advance angle relative to rotor position. Stage 2.1 must therefore sweep both the half-order ratio and the synchronous phase relationship to identify operating points that produce positive mean torque without erasing the designed signature.

- **Control modes to compare.** The minimum control set is now: native resonant signature baseline, synchronous-carrier-only baseline, hybrid idealized mode, hybrid hard-switched mode, hybrid resonant-converter mode, and matched ordinary two-phase / BLDC-style baseline.
- **Impedance matching.** The resonant stage remains the coupling interface between drive and machine. It should be tuned not just for switching convenience but for clean engagement with the machine’s preferred operating region while avoiding converter overlap with the diagnostic lines.
- **Control cleanliness.** Any sub-harmonics or super-harmonics introduced by the converter must be distinguishable from the intended machine signature; otherwise the diagnostic value of the predicted resonant structure becomes ambiguous.

## 4.5 Instrumentation requirements

The instrumentation layer is part of the architecture, not an afterthought.

- **Primary measurements.** Shaft-angle reference, torque or torque proxy, per-winding current sensing, bus voltage/current, accelerometry or vibration pickup, and temperature on magnets and windings.
- **Primary observables.**
  - mechanical line at  $\omega_{\text{mech}}$ ;
  - designed tetrad line at  $\omega_{\text{mech}}/2$ ;
  - designed tetrad sideband at  $3\omega_{\text{mech}}/2$ ;
  - converter residuals and higher-order harmonics;
  - drift of these quantities with load and temperature.
- **Core derived metrics.**
  - amplitude ratio  $A_{\omega/2}/A_{\omega}$ ;
  - conjugate-pair symmetry ratio  $A_{\omega/2}/A_{3\omega/2}$  (predicted = 1 under ideal drive);
  - linewidth and phase stability of the  $\omega/2$  and  $3\omega/2$  components;
  - input power, useful output, and conventional efficiency map;
  - repeatability across repeated sweeps and fault injections.

## 5. Research hypotheses, observables, and decision criteria

The present paper is most valuable where it states risky, measurable expectations. This section therefore frames the concept as a research program with explicit observables and decision rules, now separated by operating regime where needed.

### 5.1 Architecture and regime hypothesis

The first hypothesis is that the resonant engine should be treated as **one architecture supporting two operating regimes**, not as two different machines.

The native resonant regime is the correct regime for asking whether the architecture is genuinely distinct from ordinary two-phase commutation and whether the half-order / two-turn logic leaves measurable traces. The hybrid motoring regime is the correct regime for asking whether

the same architecture can produce practical shaft work, efficiency maps, and a commercially meaningful operating envelope.

**Primary measurements.** Back-EMF shape, inductance profile versus angle, current response, mean torque, torque ripple, spectral content, bus power, and efficiency maps for both regimes under matched hardware assumptions.

**Decision criterion.** If the architecture only behaves distinctly in non-motoring conditions and loses all distinctive behavior as soon as practical motoring control is added, then the case for the resonant engine as a distinct machine class weakens substantially. If, however, the hybrid regime preserves a measurable resonant signature while delivering practical torque, then the architecture remains distinct even if the pure native regime is not itself commercially sufficient.

## 5.2 Native resonant operating-ratio and signature hypothesis

The second hypothesis is that the architecture has a preferred native resonant operating region near

$$\omega_{\text{swap}} = \omega_{\text{mech}}/2.$$

In the native regime, the expected evidence is not a single scalar efficiency peak alone, but a cluster of behaviors: cleaner current waveforms, more stable phase relation, narrower half-order spectral content, and the appearance of the structured canonical three-line signature predicted by Appendix A.

The analytical basis for this signature remains the Stage 1 symbolic model. Substituting the canonical alternating currents at  $\omega_{\text{swap}} = \omega_{\text{mech}}/2$  into the total torque expression for a PM-biased rotor with two anti-phase stator winding sets yields, under complex-exponential decomposition, three non-zero spectral lines:

- a **tetrad line** at  $\omega_{\text{mech}}/2$ ;
- the **mechanical line** at  $\omega_{\text{mech}}$ ; and
- a **tetrad sideband** at  $3\omega_{\text{mech}}/2$ , with the outer pair matched in amplitude under canonical ideal drive.

An early Stage 2 validation pass reproduced these analytical amplitudes exactly under canonical idealized conditions. That result strengthens the status of Appendix A as a valid **native resonant signature baseline**. At the same time, the same Stage 2 pass showed that the canonical half-order current family produces near-zero mean torque. The correct interpretation is therefore not that the Stage 1 currents are wrong, but that they define the native resonant regime more cleanly than they define a practical motoring controller.

**Primary measurements.** Ratio sweep of  $\omega_{\text{swap}}/\omega_{\text{mech}}$ , input power, output torque/speed, current spectra, vibration spectra, and temperature in the native resonant mode.

**Decision criterion.** If no distinctive operating region appears near the half-order relation after control artifacts are accounted for, or if the resonant signature cannot be separated from converter and mechanical artifacts, then the 720° / half-order interpretation should be downgraded and the concept re-expressed in more conventional commutation terms. The operating-ratio hypothesis should therefore be read as a search for the machine’s preferred flow state, not merely as a search for a single scalar efficiency peak.

## 5.2A Preferred operating state (“flow”) as the engineering objective

The resonant engine should not be understood as seeking a single scalar optimum such as maximum rated-point efficiency alone. Its deeper engineering objective is to create and maintain a **preferred operating state** — here termed **flow** — in which magnetic closure,  $\alpha/\beta$  alternation, phase relation, torque production, and converter action remain mutually coherent. In that state, the machine is expected to exhibit a cluster of favorable behaviors rather than one isolated peak: cleaner current waveforms, narrower spectral content, more stable phase relation, improved load response, and potentially flatter efficiency across the operating envelope. This interpretation is already implicit in the program’s emphasis on a preferred operating region near  $\omega_{\text{swap}} = \omega_{\text{mech}}/2$ , on clean engagement between converter and machine, and on using spectral structure as a diagnostic of operating quality rather than as a decorative by-product. The broader E1P-theoretic reading of this operating state — the interpretation of the machine’s preferred productive regime in tetrad-cycle terms — is developed in the companion paper *Solar Systems as Resonant Engines* (Resonant Institute, 2026); the present paper takes the engineering consequences as its subject.

The design consequence for this machine is direct. It should be engineered so that differentiated regions are not merely alternated, but held in productive tension by an integrating interaction zone and a governor capable of restoring that relation when it drifts. Put differently: the design problem is not simply to alternate states, but to sustain the in-between field relationship that makes those states useful.

Low-speed operation is of particular interest within this framework, but it should not be treated as automatically equivalent to higher energy efficiency. The more defensible claim is narrower: low speed is the regime in which the resonant architecture is most likely to translate its coherence and tuning advantages into **better torque-per-unit-current, cleaner control, and stronger duty-cycle efficiency**, because resonant tuning is easier there and conventional PMSM control is relatively disadvantaged. Whether this becomes a net energy-efficiency advantage must still be determined empirically through matched efficiency maps against PMSM and SRM baselines. Low speed is therefore the most promising **discovery regime**, not a guaranteed efficiency regime.

This leads directly to the central architectural question of the program: whether the coherence architecture adds enough real advantage to justify the resonant design as a distinct machine class. The coherence model is useful only if it improves the machine in measurable ways that conventional additive loss accounting and ordinary commutation already do not explain — for example, flatter efficiency across load range, stronger low-speed torque density, better detuning resilience, greater thermal stability, or diagnostically useful spectral observability. If those effects fail to appear under matched baseline comparison, then coherence may remain a descriptive language for good operation, but it should not be promoted as a distinct performance model or as a sufficient justification for the resonant architecture.

Accordingly, the resonant engine’s design problem can be stated more clearly as an exercise in **engineering flow**. The goal is not merely to produce torque, nor merely to preserve a half-order signature, but to shape rotor bias,  $\alpha/\beta$  geometry, converter timing, and control law so that the machine enters and remains in its preferred coherent state under load. The central engineering objective is therefore not merely to discover the machine’s preferred operating state, but to design geometry, materials, conversion, and control so that this state can be entered quickly, held robustly, and recovered repeatedly under real operating disturbances. In that reading, torque,

efficiency flatness, thermal resilience, and self-diagnosis are not separate objectives competing for attention; they are different measurable consequences of whether the machine has successfully achieved and held flow. The resonant architecture is sustained only if that preferred state proves operationally valuable enough to outweigh the added complexity of dual windings, resonant conversion, and tighter control requirements.

### 5.3 Hybrid motoring-control hypothesis

The third hypothesis is that the architecture can be made to motor efficiently **without sacrificing its distinctive resonant signature**. More specifically, the working claim is that a rotor-synchronous torque carrier plus a superposed half-order  $\alpha/\beta$  envelope can produce behavior not reproducible by ordinary two-phase commutation once mean torque, efficiency, and signature are optimized together.

This is the decisive engineering question opened by the early Stage 2 pass. If the resonant engine is to become a practical machine rather than a spectral curiosity, there must exist at least one control family that satisfies all three conditions simultaneously:

1. positive mean torque;
2. preserved half-order diagnostic structure; and
3. no prohibitive efficiency collapse relative to conventional PM baselines at matched power level.

**Primary measurements.** Mean torque, torque ripple, torque-per-RMS-amp, bus power, spectral content, low-speed behavior, and efficiency maps for matched baseline machines or matched control modes.

**Decision criterion.** If the resonant overlay must be made so weak that it contributes no meaningful operational advantage, or if every hybrid operating point collapses into ordinary PM behavior with no residual signature advantage, then the case for the  $\alpha/\beta$  topology split weakens substantially.

#### 5.3.1 First Stage 2.1 result — conditions 1 and 2 numerically supported at canonical $k = 0.5$

The first Stage 2.1 kinematic hybrid sweep (Appendix C, 48-point grid over synchronous-carrier amplitude  $I_s \in [0, 5]$  A and phase advance  $\delta \in [0, 7\pi/8]$  rad at  $k = \omega_{\text{swap}}/\omega_{\text{mech}} = 0.5$ ) supports simultaneous satisfaction of conditions 1 and 2 of the hybrid motoring-control hypothesis across a broad operating plateau rather than at an isolated point. Thirty-five of forty-eight grid points satisfy both conditions jointly; at representative interior points mean torque is in the range  $[+0.01, +0.018]$  N·m with  $A(\omega_{\text{mech}}/2)$  preserved at the displayed numerical resolution. The plateau, rather than any single peak, is the load-bearing result: the hybrid layer behaves not as a fragile correction to a delicate native state, but as a broad operating region in which motoring and signature preservation coexist.

Two control-relevant ridges emerge within the plateau and are more informative than the peak-torque point.

**Diagnostic-preserving phase.** Near  $\delta \approx 45^\circ$ ,  $A(\omega_{\text{mech}}/2)$  is numerically unchanged at the displayed resolution as  $I_s$  varies across the full sweep range. The envelope and synchronous contributions to that line are orthogonal by construction at this phase, so the tetrad-line amplitude is decoupled from motoring drive. The control-architecture consequence is direct:

the machine admits an operating state in which **signature observability is independent of torque demand**. Given that the program’s value proposition depends materially on the half-order signature functioning as a continuous diagnostic of coherence state under load (§4.5, §6.3), this ridge provides a specific hybrid phase at which that diagnostic remains legible while the machine motors.

**Symmetry-preserving phase.** Near  $\delta \approx 67.5^\circ$ , the pair ratio  $A_{\omega/2}/A_{3\omega/2}$  remains within  $10^{-3}$  of unity across the full  $I_s$  sweep while positive mean torque is produced. This is the operating phase at which the full conjugate-pair symmetry of pure native operation is retained under motoring. The control-architecture consequence is that **the controller can trade torque magnitude against signature purity in a structured way** rather than choosing one to the exclusion of the other: mean torque at the symmetry-preserving ridge is within approximately 7% of the peak-torque plateau point while signature symmetry is substantially tighter. This is a tradeoff space the control law can navigate deliberately, not a forced choice.

Taken together, these two ridges suggest that the hybrid controller may be tuned not only for torque production, but for whether torque magnitude, signature strength, or signature purity is prioritized at a given operating point.

**What conditions 1 and 2 being numerically supported does and does not establish.** Coexistence of motoring and signature at canonical  $k = 0.5$  is supported by these results. Architectural irreducibility — whether the hybrid regime produces behavior not reproducible by ordinary two-phase commutation at matched RMS current and control quality — is **not yet** addressed by this sweep and requires the matched PMSM baseline comparison, which is the next Stage 2.1 deliverable. Until that comparison runs, the correct reading is *the hybrid resonant engine can motor while preserving signature* and not yet *the hybrid regime delivers something an ordinary machine cannot*.

The copper-only efficiency proxy at representative plateau points is approximately 20%; this figure is an **upper bound** on true efficiency under this idealized model, since adding iron, switching, bearing, and windage losses can only reduce the shaft-to-input ratio further. The sweep is kinematic: currents are prescribed through the two-layer drive law rather than produced by a physical converter tracking voltage-to-current through the electrical ODE. The realistic-converter test (Appendix C.3 modes 4 and 5: hybrid hard-switched, hybrid resonant-converter) remains open and is the principal empirical discriminator that Stage 2 must still deliver.

What this sweep does establish is that the zero-mean-torque finding from the original Stage 2 pass is a property of the **native-only Appendix A drive**, not of the architecture itself, and that the hybrid layer functions as a structured overlay capable of controllable tradeoffs rather than as a fragile correction. The dual-regime restructuring introduced in v0.11 is consistent with first numerical evidence. This sweep supports coexistence, not competitiveness.

### 5.3.2 Matched PMSM baseline and the geometry dependence of condition 3

The second Stage 2.1 experiment compares the hybrid regime to a well-tuned matched PMSM baseline on the same rotor bias and inductance scale, using pure q-axis field-oriented control at matched RMS current. This directly addresses condition 3 of §5.3 (efficiency vs conventional PM baseline) and the architectural-irreducibility question that §5.3.1 explicitly left open.

**The analytical mean-torque law.** Symbolic integration of the hybrid drive over one full mechanical period, using the ResonantEngine PM convention ( $\lambda_{pm,\alpha} = \Lambda \cos \theta$ ,  $\lambda_{pm,\beta} = \Lambda \cos(\theta +$

$\pi/2) = -\Lambda \sin \theta$ ), establishes that the mean torque produced by the two-layer drive is

$$\langle T \rangle = \frac{\sqrt{2}}{4} I_e I_s L_{a1} \sin\left(\delta + \frac{\pi}{4}\right).$$

This result is load-bearing for the interpretation of every subsequent hybrid sweep. The permanent-magnet flux contribution and the reluctance-only contribution *both integrate to zero* over the mechanical period under canonical symmetry; all mean torque in the hybrid regime is produced by the **three-way coupling of envelope, synchronous carrier, and saliency**. At  $I_e = 0$  or  $I_s = 0$  or  $L_{a1} = 0$ , mean torque is identically zero. The envelope is therefore not an auxiliary layer laid on top of a separate motoring mechanism — it is intrinsic to the motoring mechanism itself. The phase-advance angle  $\delta = \pi/4$  ( $45^\circ$ ) identified in §5.3.1 as the peak-plateau point is the angle that maximizes  $\sin(\delta + \pi/4)$ ; it is not an accident but the torque optimum of this specific coupling.

**The PMSM comparison at canonical parameters.** At the canonical saliency ratio  $L_{a1}/L_{a0} = 2$  used in the §5.3.1 sweep, the hybrid regime at its peak-plateau point ( $I_s = I_e = 5$  A,  $\delta = 45^\circ$ ) produces  $\langle T \rangle = 0.0177$  N·m against the matched PMSM’s  $\langle T \rangle = 0.2646$  N·m at the same RMS current of 6.614 A. That is 6.8% of the PMSM’s mean torque at matched thermal budget, or a factor of approximately  $15\times$  in torque-per-amp. Condition 3 of §5.3 in its strongest reading — “no prohibitive efficiency collapse relative to conventional PM baselines at matched power level” — **fails at canonical parameters by this measure**.

**Condition 3 depends strongly on saliency, not on control.** A saliency sweep at the same peak-plateau operating point ( $I_e = I_s = 5$  A,  $\delta = 45^\circ$ ) across  $L_{a1}/L_{a0} \in \{2, 3, 5, 10\}$  shows that the torque ratio against the matched PMSM rises monotonically with saliency contrast:

$L_{a1}/L_{a0}$	Hybrid $\langle T \rangle$ (N·m)	Hybrid / PMSM torque	Hybrid torque/amp (N·m/A)	$A(\omega/2)$	Pair ratio
2	0.0177	6.7%	0.00267	0.0801	0.919
3	0.0265	10.0%	0.00401	0.0850	0.885
5	0.0442	16.7%	0.00668	0.0954	0.831
10	0.0884	33.4%	0.01336	0.1231	0.748

The linear scaling of  $\langle T \rangle$  with  $L_{a1}$  follows directly from the analytical law above and confirms that **geometry — not control tuning — is the primary lever for condition 3**. The present canonical parameterization is not torque-competitive with a PMSM, but the gap narrows materially as saliency contrast increases.

**A three-objective trade space.** The saliency sweep also reveals that torque, signature amplitude, and signature symmetry are not independently tunable. Stronger saliency increases torque (proportional to  $L_{a1}$ ) *and* increases signature amplitude  $A(\omega_{\text{mech}}/2)$  (from 0.080 to 0.123 across the sweep), *but* degrades conjugate-pair symmetry (ratio from 0.919 to 0.748). The canonical symmetric pair-ratio = 1 derivation of Appendix A holds only in the limit where the reluctance contribution to  $A(\omega/2)$  and  $A(3\omega/2)$  is small relative to the PM contribution; at stronger saliency the reluctance term grows faster than the PM term and the balance shifts. This is not an artifact — it is the physics of the coupling. Geometry selection is therefore a

three-objective optimization, not a single lever: **torque-per-amp**, **signature strength**, and **signature symmetry** all respond to saliency but not in the same direction.

**Ceiling on the single-lever strategy.** Linear extrapolation of the torque ratio to parity with the PMSM requires  $L_{a1}/L_{a0}$  on the order of 30, which is not physically credible under the present lumped-inductance model — it implies a saliency modulation larger than the mean inductance, i.e., regions of the rotation where self-inductance would be negative. The practical ceiling on geometry-only closure of the torque gap is therefore well below parity. The architecture can be made substantially more actuator-competitive by geometry, but it cannot be made PMSM-equivalent by geometry alone.

**What §5.3.2 closes and what it leaves open.** The architectural-irreducibility question is now closed in both directions. On one hand, the PMSM produces  $A(\omega_{\text{mech}}/2) < 3 \times 10^{-10}$  N·m across the entire baseline sweep — the tetrad signature is unreachable to any PMSM drive because no PMSM current contains the  $\omega_{\text{mech}}/2$  frequency. On the other hand, the analytical law above establishes that the motoring mechanism itself — three-way envelope-synchronous-saliency coupling — is structurally distinct from standard q-axis field-oriented control. The resonant engine and the PMSM are therefore architecturally irreducible to each other in both directions: neither can emulate the other’s operating mode. What §5.3.2 leaves open is the condition-3 quantitative question: whether saliency-optimized geometry under physical inductance constraints (strictly positive self-inductance across the full mechanical period, realistic magnetic materials, manufacturable pole geometry) can reach a torque ratio that qualifies as “no prohibitive efficiency collapse” under any reasonable reading. Resolution requires the FEA work package (§WP1, Stage 3), and specifically a physically-constrained geometry sweep tracking all three objectives simultaneously rather than a free  $L_{a1}$  multiplier.

**Positioning consequence.** The PMSM comparison result strengthens rather than weakens the architecture’s distinct value proposition, but it relocates where that value lives. The resonant engine is not a PMSM competitor on torque-per-amp at the tested saliency levels and likely cannot be made one through geometry alone. Its unique architectural capability is the **coupling between motoring and signature**: the two are consequences of the same saliency-mediated mechanism and cannot be separated in operation. For applications where that coupling is the value — diagnostic-critical servos, motor-as-sensor robotics, active dampers with structural state reporting, systems where variable-load behavior and duty-cycle coherence matter more than peak torque-per-amp — the resonant engine is architecturally distinct in a way no PMSM can match. §6.5 already identifies this application space; §5.3.2 establishes the architectural basis for it.

## 5.4 Cross-scale coherence hypothesis

The fourth hypothesis is that performance is materially constrained by interactions across scales: magnetic material behavior, rotor geometry, air-gap quality, winding layout, converter timing, thermal stability, and mechanical compliance.

The multiplicative expression

$$\eta_{\text{max}} \approx \prod_i \eta_i^{\text{coh}}$$

should be treated as a research heuristic, not a finished model. Its purpose is to force the



program to test whether weak links compound rather than remain isolated.

**Primary measurements.** Temperature sweep, deliberate phase jitter, controlled gap variation, rotor-material comparison, and repeated load sweeps under matched control conditions in both operating regimes.

**Decision criterion.** If ordinary additive loss accounting explains the data fully and joint optimization shows no threshold-like or multiplicative effects, then the coherence framing may still be useful descriptively but should not be promoted as a distinct performance model.

## 5.5 Prototype decision gates

A first prototype need not be efficient to be valuable. It only needs to answer the following questions clearly.

**Gate 1: state distinction.** Are  $\alpha$  and  $\beta$  measurably distinct electrical and magnetic states rather than relabelings of the same machine behavior?

**Gate 2: native resonant operating region.** Does a reproducible regime appear near  $\omega_{\text{swap}}/\omega_{\text{mech}} \approx 0.5$  when the machine is operated in native resonant mode?

**Gate 3: diagnostic separability.** Can the resonant signature be separated from converter artifacts and ordinary machine faults?

**Gate 4: hybrid motoring viability.** Does at least one hybrid mode produce positive mean torque without erasing the resonant signature?

**Gate 5: load and detuning behavior.** Do load changes, thermal drift, and intentional detuning degrade the native and hybrid regimes in interpretable ways?

**Gate 6: go/no-go for the next build.** After Gates 1–5, is there enough irreducible evidence to justify optimization of geometry and materials, or should the architecture be revised before a second prototype?

## 6. Operational characteristics and application domains

This section is included to locate the concept commercially and operationally. The characteristics described are predicted from the architecture rather than claimed as achieved performance. They are organized here by **native resonant**, **hybrid motoring**, and **shared** benefits so that the paper can preserve both the original v0.4 proposition and the later commercialization-oriented benefits without conflating them. In the intended practical engine, these benefit classes are not expected to appear in isolation: the commercial target is simultaneous operation in which the hybrid motoring layer carries shaft work while the native resonant layer remains active enough to preserve the signature-driven and envelope-performance advantages. Several of the following characteristics are best understood as consequences of how successfully the machine can enter and hold its preferred coherent operating state, rather than as independent benefits that arise in isolation.

### 6.1 Benefits strongest in the native resonant regime

**Architectural distinctiveness.** The native resonant regime is where the resonant engine is most clearly not just a conventional PM machine with an added control layer. Here the  $\alpha/\beta$

alternation is primary, the half-order regime is most visible, and the EIP-derived two-turn logic is being tested in its clearest machine form.

**Cleanest test of the 720° / half-order proposition.** If the engine has a genuine two-turn operating law, it should show up most clearly in the native resonant regime, where role-swap rather than synchronous torque production is doing the primary structural work.

**Strongest diagnostic identity.** The canonical three-line signature, and especially the matched outer pair under idealized drive, belongs first to the native resonant regime. This is the regime in which the machine is most legible as a new class rather than as an optimized variant of a familiar class.

## 6.2 Benefits strongest in the hybrid motoring regime

**Positive mean torque and conventional efficiency maps.** The hybrid motoring regime is where the machine becomes comparable to PMSM, BLDC-style, and SRM baselines in the ordinary engineering sense. This is the regime in which shaft work, efficiency maps, torque-per-amp, and power-density tradeoffs can be measured honestly.

**Operational efficiency across the envelope.** The strongest efficiency claim remains not higher rated-point peak alone, but improved **operational efficiency across the envelope**. If the resonant overlay can be kept shallow while still providing its intended benefits, the hybrid machine may sustain a flatter efficiency curve across load range.

*Hypothesis:* the resonant engine exhibits a flatter efficiency-versus-load curve than a matched conventional PMSM baseline under variable-duty operation.

*Primary measurements:* efficiency map across the full load and speed envelope, compared against baseline machines under matched test conditions.

*Decision criterion:* if the efficiency curve shape is statistically indistinguishable from the baseline across load sweeps, the structural-flatness claim is not supported.

**Low-speed torque density.** Parametric resonant operation remains favourable at low mechanical speed, but any low-speed advantage must now come from the interaction of the resonant envelope with a practical motoring carrier, not from the envelope in isolation.

*Hypothesis:* the resonant engine delivers SRM-comparable low-speed torque density without SRM-class acoustic or ripple penalties.

*Primary measurements:* torque-per-unit-current at specified low-speed operating points, torque ripple spectrum, acoustic pressure, comparison against SRM and PMSM baselines.

*Decision criterion:* if low-speed torque density matches PMSM behavior rather than SRM behavior, or if the resonant overlay adds more loss than torque quality, the low-speed advantage is not supported.

## 6.3 Benefits that can survive in both regimes

**Tonal rather than broadband acoustic signature.** Conventional PMSMs radiate at integer multiples of electrical frequency; switched-reluctance machines radiate broadband noise from abrupt commutation. The resonant engine's dominant radiation is still expected to concentrate near the canonical resonant lines if the alternation remains clean.

*Hypothesis:* acoustic radiation concentrates in the predicted resonant structure rather than a broadband distribution.

*Primary measurements:* acoustic spectrum characterization under representative operating conditions, compared against PMSM and SRM baselines.

*Decision criterion:* if acoustic radiation is broadband, dominated by integer harmonics not present in the Stage 1 prediction, or lacks the expected resonant structure, this characteristic is not supported.

**Continuous structural self-diagnosis.** The  $\omega_{\text{mech}}/2$  line and its sidebands may carry scale-resolved diagnostic information about which coherence scale — grain, magnet, gap, winding, drive, thermal, mechanical — is currently bottlenecking. Whether the engine is run in native or hybrid mode, this remains one of the strongest commercial benefits if it can be made robust.

**Graceful degradation under winding failure.** Two winding sets mean single-set failure can degrade performance without killing operation. In native mode this is an architectural redundancy question; in hybrid mode it becomes an availability and service-life question.

**Thermal coherence management in real time.** SmCo rotor bias plus remainder-diagnostic control could support closed-loop thermal coherence tracking, replacing open-loop derating tables with coherence-based derating. This remains especially relevant in aerospace actuators, downhole tooling, and high-power-density applications where thermal management dominates design.

## 6.4 Characteristics contingent on the cross-scale coherence hypothesis

The following claims depend on §5.4 holding in its multiplicative form. They are the strongest claims in the program and the most likely to require qualification or falsification.

**Efficiency ceiling exceeding best-in-class PMSMs across the load curve.** If multiplicative coherence holds, an engine that co-optimises all scales could eventually outperform machines optimised one-scale-at-a-time. This is not assumed and should not be claimed without data.

**Motor-as-sensor applications.** Fine-grained self-diagnosis could enable application classes where motor behavior is part of the control loop of something larger — collaborative robotics where motor spectra reveal physical contact, surgical robotics where motor dynamics reveal tissue properties, precision servo systems where positioning is inferred from motor signatures rather than external sensors.

## 6.5 Application domains where the combination matters

The resonant engine is unlikely to displace commodity induction motors or cost-optimized PMSMs in general-purpose applications. Its likely commercial path lies in domains where the characteristics combine.

The §5.3.2 analytical result sharpens what is being combined. The architecture’s motoring mechanism and its diagnostic signature are not two independent features that happen to coexist in the same machine: they are consequences of a single saliency-mediated three-way coupling between envelope, synchronous carrier, and reluctance modulation, which produces both the mean torque and the tetrad line structure. **Motor-sensor coupling is therefore the architectural primitive the matched PMSM comparison establishes as irreducible**, not merely an availability of a secondary diagnostic output. The family-level reading of why motor-sensor coupling is architectural rather than incidental — its placement within the tetrad-cycle specification’s fourth precondition, structured remainder as primary observable — is developed in the companion paper *Solar Systems as Resonant Engines* (Resonant Institute,

2026). The present section takes the engineering consequence as given: application domains where the coupling itself is the value are where this machine is most likely to be a superior choice.

- **Variable-load systems.** Traction, collaborative robotics, HVAC, pumps, compressors. Duty-cycle coherence matters more than peak torque-per-amp.
- **Diagnostic-critical domains.** Aerospace, medical, nuclear, defense. Continuous structural self-diagnosis is intrinsic to operation rather than added through extra instrumentation.
- **Acoustic-critical domains.** Submarines, medical imaging suites, premium consumer appliances. Tonal rather than broadband radiation follows from the coupling structure itself.
- **Motor-as-sensor systems.** Collaborative and surgical robotics, precision servo, haptic systems. The tetrad line reports rotor and load state continuously; this is the clearest application class for the coupling primitive.
- **Instrumented active-load systems.** Active dampers, precision flywheel storage, haptic feedback actuators. These applications treat the motor-sensor coupling as the product rather than as a secondary feature.
- **Demonstrator and research use.** Validating E1P’s predictive reach on a physical system whose behavior can be measured against specific quantitative signatures.

## 6.6 What is not improved

- **Manufacturing cost.** Dual-wound stator, precision  $\alpha/\beta$  geometric relationship, SmCo magnets, and resonant converter all cost more than their PMSM equivalents.
- **Drop-in replacement capability.** Control architecture, drive electronics, and diagnostic integration are all different.
- **Guaranteed peak efficiency at the rated operating point.** Expected advantages manifest across the load curve and operating envelope, not necessarily at the peak.
- **Independence of characteristics.** Several of the above trade against each other. Stronger resonant signature may cost efficiency; higher diagnostic resolution may cost sensor or thermal budget.

## 7. Related machine families and prior-art context

### 7.1 Purpose of the comparison

This section is included to locate the research program in the existing machine landscape and to define meaningful experimental baselines. At this stage it should not be read primarily as a legal novelty argument. The safest current statement is that the initial survey found multiple partial precedents but did not locate an exact match for the full architecture under study.

### 7.2 Closest partial precedents

**Fam (1971), US Patent 3,716,734, “Parametric Motor.”**

Still the closest precedent found for the two-stationary-circuit idea. Fam uses two stationary magnetic circuits sharing a rotor, with one winding supply-driven and the other capacitor-tuned and parametrically excited. It remains the strongest comparison on the parametric-motor axis.

**Pollock and Wallace (1999), “The Flux Switching Motor, a DC Motor without**

### **Magnets or Brushes.”**

Relevant on the alternating-stator-state axis. It differs in being wound-field rather than PM-biased and in not being organized around a designed half-order operating condition.

### **Yazdan, Atiq, Kwon et al. (2019), dual-stator ironless PM machine.**

Still the strongest precedent found on the alternating-winding plus ironless-PM axis. It is valuable as an experimental comparison class even if the operating rationale differs from the one proposed here.

### **Cap (1986), “Parametric Electric Machine,” and the Mandelstam-Papalexi lineage.**

These works remain important because they anchor the parametric-machine tradition and remind us that resonant behavior in rotating electromechanical systems has prior history.

### **Brushless wound-rotor synchronous machines with sub-harmonic stator excitation.**

These are strong comparisons on the “two winding sets plus half-order content” axis, even though the mechanism there is spatial-harmonic rather than temporal alternation between two stator roles.

### **Hybrid stepper and PM-biased reluctance families.**

These remain important comparison classes because they combine PM rotor bias with alternating phase excitation and therefore provide realistic experimental baselines for what may or may not be genuinely new in the present concept.

## **7.3 Where the current concept appears distinct**

The current architecture appears provisionally distinct in the following combination of features:

1. a PM-biased rotor used primarily as a stable magnetic substrate;
2. two stator winding sets assigned deliberately different magnetic-circuit roles rather than treated as ordinary commutation phases;
3. a resonant drive used as both power interface and alternation mechanism;
4. a research emphasis on a designed half-order operating signature; and
5. a development framework that treats cross-scale coherence as a first-order design variable.

That statement remains provisional pending broader literature and patent work.

## **7.4 What remains open in the prior-art picture**

The initial sweep still leaves open several important areas: Russian-language parametric-machine literature after Mandelstam-Papalexi, Japanese post-parametron motor work, and Chinese-language patents in dual-winding, ironless, and Halbach-adjacent machine spaces. A targeted CPC-class H02K search is still recommended before any formal novelty claim is made.

## **7.5 What this document does not claim**

This paper does **not** claim:

- best-in-class efficiency at rated point;
- that the canonical half-order envelope, by itself, already constitutes a practical motoring controller;
- violation of any conservation law;
- novelty in magnets, sensors, switches, or winding conductors as individual components;
- immediate manufacturability or cost competitiveness;

- completion of the literature and patent search required for formal novelty assertions.

The role of the prior-art section at this stage is to sharpen the research program, not to overclaim what has already been established. ## 8. Physical invariants and non-goals

The research program is intended to remain inside standard physical constraints at all times.

- **Energy conservation.** No free-energy claim is made or implied. Any useful machine in this program must remain strictly within ordinary conservation bounds.
- **Charge continuity.** Current continuity and field evolution remain governed by standard electromagnetic relations.
- **Magnetic-flux closure.** The constraint  $\nabla \cdot \mathbf{B} = 0$  is treated as a design constraint, not an optional interpretive flourish.
- **Second-law limits.** Thermal losses, friction, converter losses, and other irreversibilities remain real and must be measured explicitly.

The non-goals are equally important. The present program is not trying to bypass conservation, replace standard machine theory wholesale, or declare performance superiority before data exist. Its purpose is narrower: to determine whether this architecture yields measurable, useful behavior that warrants further development.

## 9. Development priorities and work packages

The next phase of work should be organized around a small number of tightly coupled work packages.

### 9.1 WP1 — $\alpha/\beta$ stator geometry

Define at least one manufacturable pair of  $\alpha$  and  $\beta$  winding/topology layouts that are measurably distinct in magnetic-circuit behavior. This is the highest-priority task because it sets the inductance profile, the torque-production mechanism, and the converter requirements.

**Deliverables:** geometry candidates, inductance-versus-angle maps, expected back-EMF behavior, and a justification for why the two states are genuinely distinct.

### 9.2 WP2 — Rotor bias material and layout

Select a rotor magnet material and arrangement that maximize thermal stability and repeatability of the standing magnetic bias while remaining buildable for bench prototypes.

**Deliverables:** candidate material shortlist, thermal sensitivity comparison, and at least one baseline rotor layout suitable for rapid prototyping.

### 9.3 WP3 — Resonant converter and control strategy

Choose the simplest converter architecture that can execute the  $\alpha/\beta$  alternation cleanly while keeping converter-generated half-order artifacts distinguishable from machine behavior.

The work package is now explicitly two-layered: define a practical **rotor-synchronous torque carrier** and then define the smallest **resonant  $\alpha/\beta$  envelope** that preserves the intended signature and operational advantages.

**Deliverables:** control modes for canonical signature baseline, synchronous-carrier-only baseline, hybrid idealized mode, hybrid hard-switched mode, hybrid resonant-converter mode, and matched ordinary two-phase / BLDC-style operation; phase-advance plan; timing plan; instrumentation hooks for synchronized logging; and a first comparison of bus power, mean torque, and signature retention across modes. ### 9.4 WP4 — Instrumentation and signal processing

Design the measurement chain early. A weak concept can look persuasive without instrumentation, and a good concept can be lost without it.

**Deliverables:** synchronized data acquisition for shaft angle, current, voltage, vibration, torque proxy, and temperature; repeatable FFT and order-tracking workflow; and baseline fault-injection procedures.

## 9.5 WP5 — Modeling and comparison baselines

Maintain a modeling stack that runs in parallel with hardware development and always includes comparison baselines from conventional machine operation.

**Deliverables:** lumped magnetic-circuit model; Stage 2.1 hybrid-control sweep over carrier amplitude, envelope depth, phase advance, and detuning ratio; converter-machine co-simulation; one or more FEA studies; matched comparison cases using synchronous-only, ordinary two-phase, BLDC-style, and SRM-style operation; first conventional efficiency maps; first duty-cycle efficiency estimate; first thermal derating comparison; and investor-facing summary tables translating technical results into mean torque, efficiency, signature strength, and baseline deltas.

# 10. Experimental roadmap

## 10.1 Modeling sequence

The recommended modeling sequence is now:

1. **Lumped architecture model.** Establish whether the proposed  $\alpha/\beta$  states are meaningfully distinct in inductance, flux linkage, and expected torque interaction.
2. **Stage 2.1 hybrid-control sweep.** Identify at least one current family that simultaneously produces positive mean torque, preserves the half-order signature, and avoids unacceptable efficiency collapse.
3. **Converter-machine co-simulation.** Evaluate whether the proposed hybrid half-order operation survives realistic switching, parasitics, and thermal drift.
4. **Magnetic field model / FEA.** Check closure paths, leakage, air-gap sensitivity, and rotor/stator interaction for at least one concrete geometry chosen from the promising Stage 2.1 control region.
5. **Spectral-analysis pipeline.** Build the signal-processing workflow before hardware so that the same metrics can be applied immediately to prototype data. ### 10.2 Prototype sequence

A staged prototype path is preferable to a single ambitious build.

1. **Prototype 0 — static characterization rig.** Use stator coupons, a controllable magnetic path, or a slow mechanical rig to verify that  $\alpha$  and  $\beta$  produce genuinely different magnetic responses.
2. **Prototype 1 — benchtop rotary demonstrator.** Prioritize instrumentation and operating clarity over power density or packaging.

3. **Prototype 2 — optimized research platform.** Only after the half-order operating claim and diagnostic separability are supported should the program invest in geometry and materials optimization.

### 10.3 Core test matrix

Every serious prototype should be exercised under the same minimum test matrix:

- canonical signature baseline (Appendix A currents);
- synchronous-carrier-only baseline;
- hybrid idealized mode;
- hybrid  $\alpha/\beta$  with hard switching;
- hybrid  $\alpha/\beta$  with resonant drive;
- matched ordinary two-phase / BLDC-style baseline;
- ratio sweep of  $\omega_{\text{swap}}/\omega_{\text{mech}}$ ;
- synchronous phase-advance sweep;
- envelope-depth sweep;
- load sweep;
- thermal soak;
- winding-disable / graceful-degradation test;
- deliberate detuning and fault injection.

This matrix is what makes the results interpretable rather than anecdotal. ### 10.4 How to interpret outcomes

A useful outcome does not have to be a strong success. Three classes of result are all valuable:

- **Positive result.** A reproducible half-order operating region appears, is diagnostically separable, and survives baseline comparison.
- **Mixed result.** Some signatures appear, but they collapse under better controls or reduce to known machine behavior. This still helps prune the concept and refine the next build.
- **Negative result.** The  $\alpha/\beta$  distinction does not survive measurement, or the half-order claim fails under baseline comparison. This is still progress because it identifies which conceptual branch should be dropped.

### 10.5 Value to the broader research program

Even if a specific prototype fails, the program can still produce durable outputs: better understanding of which magnetic topologies are worth pursuing, a cleaner measurement methodology for half-order behavior in rotating machines, and a sharper distinction between what belongs to the architecture itself and what belongs only to the current EIP interpretation.

## 11. Conclusion

This draft should be read as a research framework for developing a resonant engine, not as a completed theoretical defense and not as a proof of performance. Its main contribution is to make the program more rigorous while preserving the strongest elements of both the earlier and later drafts: it defines the candidate architecture, states the measurable hypotheses, specifies the comparison baselines, and organizes the next engineering steps into explicit work packages and decision gates.



The key clarification of v0.11 is that the resonant engine should be treated as **one architecture with two operating regimes**. The native resonant regime preserves the original proposition most clearly: it is where the machine is most distinct, where the half-order / 720° logic is most visible, and where the resonant signature is tested in its cleanest form. The hybrid motoring regime is the practical engineering path: it is where the same architecture is asked to deliver positive mean torque, efficiency maps, low-speed behavior, and commercially relevant operation without surrendering its diagnostic and spectral identity. The deeper engineering objective across both regimes is to discover, enter, and hold the machine’s preferred coherent operating state. In E1P terms, the machine is best understood as **CA-seeking: AA enters CA, CC sustains CA, and AC restores CA** when disturbances degrade coherence. These regimes are analytically separable but operationally compatible: the intended efficient-engine configuration uses them **at the same time**, with the motoring layer producing mean torque and the resonant layer remaining active as a superposed structure rather than being switched off.

The concept now stands or falls on a tractable set of experimental questions. Are  $\alpha$  and  $\beta$  genuinely distinct machine states? Does a reproducible native resonant regime appear near  $\omega_{\text{swap}} = \omega_{\text{mech}}/2$ ? Can the designed resonant signature be separated from converter artifacts and ordinary faults? Does at least one hybrid mode preserve that signature while delivering useful mean torque? Do thermal drift, detuning, and load changes affect the machine in ways that reveal real cross-scale coupling? Those are the questions that can advance this engine from idea to disciplined research object.

If the answers are strong, the next step is optimization. If the answers are weak or mixed, the next step is revision. Either way, the research advances by making the development pathway explicit and measurable. At its strongest, that pathway is not simply a search for an isolated performance peak, but a search for a machine design that can enter, sustain, and recover its preferred coherent operating state for as much of the duty cycle as possible.

## Appendix A. Stage 1 symbolic derivation of the three-line signature

This appendix records the analytical derivation that underlies the refined spectral-signature hypothesis in §5.2. The goal is to make the claim self-contained in the paper: a reader should be able to see *why* a three-line spectrum with matched outer-pair amplitudes is predicted, without having to consult the digital twin code directly. ### A.1 Setup

The resonant engine is modelled as a two-winding machine on a PM-biased rotor under steady rotation  $\theta(t) = \omega_{\text{mech}} t$ . The two stator winding sets  $\alpha$  and  $\beta$  have self-inductances

$$L_{\alpha}(\theta) = L_{a0} + L_{a1} \cos(N_p \theta), \quad L_{\beta}(\theta) = L_{b0} + L_{b1} \cos(N_p \theta + \delta_{ab}),$$

and each winding links a rotor-position-dependent PM flux. The PM flux linkages with  $\alpha$  and  $\beta$  are written

$$\lambda_{pm,\alpha}(\theta) = \Lambda_{\alpha} \cos(N_p \theta), \quad \lambda_{pm,\beta}(\theta) = \Lambda_{\beta} \cos(N_p \theta + \delta_{pm}).$$

The total electromagnetic torque is the sum of reluctance, mutual, and PM-biased contributions:

$$T(\theta, i_\alpha, i_\beta) = \frac{1}{2} i_\alpha^2 \frac{dL_\alpha}{d\theta} + \frac{1}{2} i_\beta^2 \frac{dL_\beta}{d\theta} + i_\alpha i_\beta \frac{dM}{d\theta} + i_\alpha \frac{d\lambda_{pm,\alpha}}{d\theta} + i_\beta \frac{d\lambda_{pm,\beta}}{d\theta}.$$

## A.2 Idealized alternating drive at $\omega_{\text{mech}}/2$

Under the architecture's tuning rule  $\omega_{\text{swap}} = \omega_{\text{mech}}/2$ , the idealized drive alternates between  $\alpha$  and  $\beta$  at half the mechanical rotation frequency. The cleanest symbolic representation of this alternation is

$$i_\alpha(t) = \frac{I_0}{2} \left[ 1 + \cos\left(\frac{\omega_{\text{mech}}}{2}t\right) \right], \quad i_\beta(t) = \frac{I_0}{2} \left[ 1 - \cos\left(\frac{\omega_{\text{mech}}}{2}t\right) \right].$$

This satisfies the alternation condition ( $i_\alpha + i_\beta = I_0$  at all times;  $i_\alpha$  peaks when  $i_\beta$  vanishes, and vice versa) while being analytically tractable.

In v0.9, however, these currents are assigned a more precise role. They are the **canonical signature baseline** for the tetrad-cycle spectrum, not a claim that the half-order envelope by itself is already the final motoring controller. The early Stage 2 validation pass confirms that this current family reproduces the Stage 1 spectrum exactly; the same Stage 2 pass also shows that it yields near-zero mean torque under the canonical symmetric assumptions. That is why Stage 2.1 introduces a hybrid controller rather than discarding the Appendix A baseline. ###  
A.3 Canonical simplification

For the cleanest illustration of the spectral structure we examine the canonical symmetric case:

$$N_p = 1, \quad L_{b0} = L_{a0}, \quad L_{b1} = L_{a1}, \quad \delta_{ab} = \pi, \quad M = 0, \quad \Lambda_\alpha = \Lambda_\beta \equiv \Lambda, \quad \delta_{pm} = \frac{\pi}{2}.$$

The anti-phase condition  $\delta_{ab} = \pi$  is what makes  $\alpha$  and  $\beta$  genuinely distinct magnetic circuits rather than spatial shifts of the same topology: their saliency modulations are 180° opposed, so when  $\alpha$ 's inductance is maximal,  $\beta$ 's is minimal. The PM quadrature  $\delta_{pm} = \pi/2$  is the natural geometric offset for windings whose effective magnetic axes are orthogonal. Departures from these values are part of the parameter space Stage 2 will sweep; the idealized case is the analytical baseline.

Under this simplification the total torque reduces to

$$T(t) = -\frac{1}{2} L_{a1} \left[ i_\alpha^2 - i_\beta^2 \right] \sin(\omega_{\text{mech}}t) - \Lambda i_\alpha \sin(\omega_{\text{mech}}t) - \Lambda i_\beta \cos(\omega_{\text{mech}}t),$$

using  $\sin(\omega_{\text{mech}}t + \pi) = -\sin(\omega_{\text{mech}}t)$  for the  $\beta$  reluctance term and  $\sin(\omega_{\text{mech}}t + \pi/2) = \cos(\omega_{\text{mech}}t)$  for the  $\beta$  PM term.

## A.4 Product-to-sum expansion

Substituting the idealized currents and expanding the products using complex-exponential identities

$$\cos(A) \cos(B) = \frac{1}{2} [\cos(A+B) + \cos(A-B)], \quad \sin(A) \cos(B) = \frac{1}{2} [\sin(A+B) + \sin(A-B)],$$

every term in  $T(t)$  becomes a sum of pure sinusoids at frequencies that are integer multiples of  $\omega_{\text{mech}}/2$ . Collecting by frequency yields exactly three non-zero components.

### A.5 The three spectral lines

The amplitudes, from direct coefficient extraction in the complex-exponential decomposition:

$$A\left(\frac{1}{2}\omega_{\text{mech}}\right) = \frac{I_0}{4}\sqrt{I_0^2 L_{a1}^2 + 2I_0 L_{a1} \Lambda + 2\Lambda^2}$$

$$A(\omega_{\text{mech}}) = \frac{\sqrt{2} I_0 \Lambda}{2}$$

$$A\left(\frac{3}{2}\omega_{\text{mech}}\right) = \frac{I_0}{4}\sqrt{I_0^2 L_{a1}^2 + 2I_0 L_{a1} \Lambda + 2\Lambda^2}$$

All other integer-half multiples of  $\omega_{\text{mech}}$  up to  $3\omega_{\text{mech}}$  have zero amplitude in this idealized case.

### A.6 Observations that matter for the paper's claims

**The conjugate-pair symmetry is exact.** The  $\omega/2$  and  $3\omega/2$  amplitudes are identical:

$$\frac{A(\omega_{\text{mech}}/2)}{A(3\omega_{\text{mech}}/2)} = 1.$$

This is what makes the diagnostic stronger than a single half-order claim: the pair structure is a two-dimensional constraint (amplitude equality *and* specific phase relationship) rather than a single amplitude, so spurious half-order content from unrelated sources has two independent conditions to satisfy simultaneously in order to mimic the signature.

**The mechanical line is saliency-independent.**  $A(\omega_{\text{mech}})$  contains only  $\Lambda$ , not  $L_{a1}$ . The mechanical-frequency torque is the conventional PM contribution and behaves exactly as in a standard PMSM at comparable drive level — it is not the distinguishing feature. The distinguishing feature is the *pair*.

**The tetrad lines are non-zero even with no saliency.** Setting  $L_{a1} = 0$  in the formulae above gives  $A(\omega/2) = A(3\omega/2) = I_0 \Lambda \sqrt{2}/4 \neq 0$ . The tetrad signature therefore does not require a reluctance-producing geometry — it arises from the alternating excitation of PM-coupled windings. Reluctance adds to the amplitude but is not necessary for the signature to exist.

**The tetrad lines are also non-zero with no PM bias.** Setting  $\Lambda = 0$  gives  $A(\omega/2) = A(3\omega/2) = I_0^2 L_{a1}/4 \neq 0$ . The signature therefore does not require PM bias either; a pure biased-reluctance machine with alternating drive would also produce it, with quadratic rather than linear dependence on  $I_0$ . Both mechanisms contribute independently and the pair structure survives.

**Numerical confirmation.** The digital twin's Stage 1 numerical verification computed the FFT of  $T(t)$  under the same simplifications with  $I_0 = 5$  A,  $L_{a1} = 2$  mH,  $\Lambda = 0.04$  Wb,  $\omega_{\text{mech}} = 2\pi \times 50$  rad/s. The numerically extracted amplitudes at  $\omega_{\text{mech}}/2$ ,  $\omega_{\text{mech}}$ , and  $3\omega_{\text{mech}}/2$  agreed with the

analytical formulae above to 100.00% in each case; the conjugate-pair ratio was 1.000000 to the precision of the calculation.

## A.7 Scope and limits

This derivation applies strictly to the canonical symmetric case under idealized drive and lossless assumptions. The expected departures under realistic conditions, which Stage 2 and Stage 2.1 of the digital twin must quantify, include:

- Broken symmetry in the conjugate pair when  $L_{b0} \neq L_{a0}$  or  $L_{b1} \neq L_{a1}$  ( $\alpha$  and  $\beta$  not identically tuned);
- Additional sidebands when  $\delta_{ab} \neq \pi$  ( $\alpha$  and  $\beta$  not perfectly anti-phase);
- Converter switching harmonics superimposed on the three-line structure and potentially overlapping the predicted lines;
- Resistive and iron losses attenuating all lines non-uniformly;
- Multi-pole-pair ( $N_p > 1$ ) spreading the signature across  $N_p\omega_{\text{mech}}$  instead of  $\omega_{\text{mech}}$ ;
- Non-zero mutual inductance  $M \neq 0$  redistributing torque across additional frequencies;
- Synchronous carrier terms introduced intentionally in Stage 2.1 to generate positive mean torque while preserving the resonant envelope.

A further limit is now explicit. The idealized Appendix A currents do **not** by themselves constitute a full motoring controller under the canonical symmetric assumptions: they produce the three-line signature cleanly, but they also produce near-zero mean torque. This does not weaken the derivation. It clarifies its role. Appendix A establishes the resonant-engine signature in the cleanest possible form; Stage 2.1 tests whether a practical motoring controller can preserve that signature while doing useful work.

## Appendix B. Architectural family and cross-scale context

The resonant engine belongs to an architectural family whose broader cross-scale context — including its structural relation to Joseph P. Firmage’s Potentum Physics framework, the associated ORIGAMI Replication discipline as a methodological standard, and the cosmic-scale instances of the same tetrad-cycle architecture — is developed in the companion paper *Solar Systems as Resonant Engines, and Resonant Engines as Localised Solar Systems* (Resonant Institute, 2026). That paper specifies the shared architectural genus in E1P terms and locates the resonant engine as one instance within it, using the classical scholastic method of *genus proximus et differentia specifica* to discipline the cross-scale identification.

The present paper’s scope is machine-scale: architecture, hypotheses, observables, and decision criteria for the resonant engine itself. Readers interested in the broader architectural family, in the Potentum correspondence, or in the ORIGAMI methodological standard should consult the companion paper, where these topics are developed with the evidentiary standard appropriate to structural rather than engineering claims.

## Appendix C. Stage 2.1 dual-regime control and comparison study

This appendix records the revised Stage 2.1 specification that follows from the early Stage 2 validation pass. Its purpose is **not** to replace the native resonant proposition with a purely

hybrid one. Its purpose is to ensure that the digital twin can evaluate both operating regimes on the same architectural footing.

### C.1 Purpose

Stage 2.1 now has two linked jobs:

1. preserve a valid **native resonant baseline** for signature-first analysis; and
2. identify at least one **hybrid motoring control family** that produces useful shaft torque while preserving a measurable resonant signature.

### C.2 Working drive law

The simulator shall support a two-layer current family of the form

$$i_\alpha(t) = \frac{I_e}{2} [1 + \cos(\omega_{\text{swap}}t + \phi_e)] + i_{\alpha,\text{sync}}(\theta + \delta)$$

$$i_\beta(t) = \frac{I_e}{2} [1 - \cos(\omega_{\text{swap}}t + \phi_e)] + i_{\beta,\text{sync}}(\theta + \delta)$$

where  $I_e$  is the resonant-envelope amplitude,  $\phi_e$  is envelope phase,  $\delta$  is synchronous phase advance, and the synchronous terms provide the rotor-synchronous torque carrier.

The canonical Appendix A current family shall remain in the simulator unchanged as the **native resonant signature baseline**.

### C.3 Minimum simulation modes

The simulator shall support the following modes:

1. native resonant signature baseline (Appendix A currents);
2. synchronous-carrier-only PM baseline;
3. hybrid idealized mode;
4. hybrid hard-switched mode;
5. hybrid resonant-converter mode;
6. matched ordinary two-phase / BLDC-style baseline;
7. SRM-style low-speed comparison mode where relevant.

### C.4 Primary sweep variables

Stage 2.1 shall sweep:

- synchronous carrier amplitude;
- resonant-envelope amplitude  $I_e$ ;
- synchronous phase advance  $\delta$ ;
- ratio  $k = \omega_{\text{swap}}/\omega_{\text{mech}}$ ;
- envelope phase offset  $\phi_e$ ;
- $L_{b0}/L_{a0}$  and  $L_{b1}/L_{a1}$  symmetry breaking;
- $\delta_{ab}$  and  $\delta_{pm}$ ;
- mutual inductance  $M$ ;
- converter mode (idealized / hard-switched / resonant);

- temperature-dependent PM-bias drift for both SmCo and NdFeB classes.

## C.5 Metrics to report

**Native resonant metrics** -  $A(\omega_{\text{mech}}/2)$ ; -  $A(\omega_{\text{mech}})$ ; -  $A(3\omega_{\text{mech}}/2)$ ; -  $A_{\omega/2}/A_{3\omega/2}$ ; -  $A_{\omega/2}/A_{\omega}$ ; - linewidth and phase stability of the resonant pair.

**Motoring metrics** - mean torque  $\bar{T}$ ; - RMS torque; - torque ripple percentage; - output power  $\bar{T} \omega_{\text{mech}}$ .

**Electrical metrics** - RMS current per winding; - bus power; - copper-loss estimate; - core-loss estimate; - converter-loss estimate; - total simulated efficiency.

**Envelope-performance metrics** - efficiency-versus-load flatness; - low-speed torque-per-amp; - thermal derating onset; - retained torque under winding-disable mode; - signature retention under thermal drift.

## C.6 Pass criteria

Stage 2.1 shall be treated as successful only if it demonstrates both of the following classes of result:

**Native resonant pass** 1. preservation of the canonical resonant signature in the native regime; and 2. separability of that signature from converter artifacts.

**Hybrid motoring pass** 1. positive mean motoring torque under at least one hybrid mode; 2. preserved resonant diagnostic structure that remains measurable under that mode; and 3. no efficiency collapse relative to conventional PM baseline at matched power level.

A stronger success is achieved if the hybrid mode also shows flatter efficiency across load range than the PM baseline, improved low-speed torque-per-amp relative to the PMSM baseline, and retained diagnostic clarity under thermal and detuning sweeps.

## C.7 Investor-facing outputs

Stage 2.1 shall produce a summary table in the form:

**mode -> regime -> mean torque -> efficiency -> signature strength -> symmetry ratio -> baseline delta**

and a small family of standard figures:

- native-regime signature heatmaps;
- efficiency heatmaps over load and speed;
- mean-torque heatmaps over carrier amplitude and phase advance;
- signature heatmaps over detuning ratio and envelope depth;
- thermal retention plots;
- Pareto fronts comparing efficiency, torque ripple, and signature strength.

## References

*Primary framework sources:*

- Resonant Institute (2026). *Energetic First Principles: The Fundamental Energetic View of Reality — An E1P Primer*. [Primer.]
- Resonant Institute (2026). *E1P as the First Principles Creating and Governing Electromagnetism*. [EM preprint.]

*Flux-switching permanent-magnet machines:*

- Hoang, E., Ben-Ahmed, A.H., Lucidarme, J. (1997). “Switching Flux Permanent Magnet Polyphased Synchronous Machines.” Proc. EPE’97, Trondheim, vol. 3, pp. 903–908.
- Zhu, Z.Q. et al. (2005). IEEE Trans. Magn. 41(11):4277–4287. DOI 10.1109/TMAG.2005.854441.
- Chen, J.T., Zhu, Z.Q., Howe, D. (2008). IEEE Trans. Magn. 44(12):4659–4667. DOI 10.1109/TMAG.2008.2004264.
- Hua, W., Cheng, M., Zhu, Z.Q., Howe, D. (2008). IEEE Trans. Energy Convers. 23(3):727–733.
- Cheng, M., Hua, W., Zhang, J., Zhao, W. (2011). IEEE Trans. Ind. Electron. 58(11):5087–5101. DOI 10.1109/TIE.2011.2123853.
- Pollock, C., Wallace, M. (1999). “The Flux Switching Motor, a DC Motor without Magnets or Brushes.” IAS’99 Conf. Rec., vol. 3, pp. 1980–1987. DOI 10.1109/IAS.1999.806009.

*Dual-wound and multiphase synchronous machines:*

- Levi, E. (2008). IEEE Trans. Ind. Electron. 55(5):1893–1909. DOI 10.1109/TIE.2008.918488.
- Zhao, Y., Lipo, T.A. (1995). IEEE Trans. Ind. Appl. 31(5):1100–1109. DOI 10.1109/28.464525.
- Bojoi, R. et al. (2003). IEEE Trans. Ind. Appl. 39(3):752–760.
- Levi, E., Barrero, F., Duran, M. (2016). IEEE Trans. Ind. Electron. 63(1):429–432.
- Barcaro, M., Bianchi, N., Magnussen, F. (2011). IEEE Trans. Ind. Electron. 58(9):3825–3832.
- Rehman, Z. et al. (2022). World Electric Vehicle Journal 13(1):16.
- Ayub, M. et al. (2023). Mathematics 11(5):1117.

*Parametric electromechanical machines:*

- Mandelstam, L.I., Papalexi, N.D. (1934). *Zh. Eksp. Teor. Fiz.* 4. [Foundational rotary parametric generator.]
- Pechenkin, A. (2019). *L.I. Mandelstam and His School in Physics*. Springer. DOI 10.1007/978-3-030-17685-3.
- Fam, W.Z. (1971). US Patent 3,716,734, “Parametric Motor.”
- Pickup, I.E.D. (1980). “Principles of Operation of the Parametric Reluctance Motor.” *Electric Machines & Power Systems* 5(6).
- Cap, F. (1986). US Patent 4,622,510, “Parametric Electric Machine.”
- Goto, E. (1959). “The Parametron, a Digital Computing Element Which Utilizes Parametric Oscillation.” Proc. IRE 47(8):1304–1316.

*PM-biased reluctance machines, SRM, and stepper motors:*

- Liao, Y., Liang, F., Lipo, T.A. (1995). IEEE Trans. Ind. Appl. 31(5):1069–1078. DOI 10.1109/28.464521.
- Deodhar, R.P., Andersson, S., Boldea, I., Miller, T.J.E. (1997). IEEE Trans. Ind. Appl. 33(4):925–934. DOI 10.1109/28.605734.
- Vagati, A. et al. (1998). IEEE Trans. Ind. Appl. 34(4):758–765. DOI 10.1109/28.703969.
- Lawrenson, P.J. et al. (1980). IEE Proc. B 127(4):253–265. DOI 10.1049/ip-b.1980.0034.

- Miller, T.J.E. (1993). *Switched Reluctance Motors and Their Control*. Oxford University Press / Magna Physics. ISBN 0-19-859387-2.
- Krishnan, R. (2001). *Switched Reluctance Motor Drives*. CRC Press. ISBN 0-8493-0838-0.

*Resonant converter topologies for motor drives:*

- Divan, D.M. (1986). “The Resonant DC Link Converter.” IAS Conf. Rec., pp. 648–656. Journal version: IEEE Trans. Ind. Appl. 25(2), 1989.
- Steigerwald, R.L. (1988). IEEE Trans. Power Electron. 3(2):174–182. DOI 10.1109/63.4347.
- Divan, D.M., Skibinski, G. (1989). IEEE Trans. Ind. Appl. 25(4):634–643.
- De Doncker, R.W.A.A., Divan, D.M., Kheraluwala, M.H. (1991). IEEE Trans. Ind. Appl. 27(1):63–73.
- Park, S.S., Lipo, T.A. (1992). “New Series Resonant Converter for Variable Reluctance Motor Drive.” PESC’92, vol. 2, pp. 833–838.

*Ironless, Halbach, and axial-flux machines:*

- Halbach, K. (1980). Nucl. Instrum. Methods 169(1):1–10. DOI 10.1016/0029-554X(80)90094-4.
- Zhu, Z.Q., Howe, D. (2001). IEE Proc. Electr. Power Appl. 148(4):299–308. DOI 10.1049/ip-epa:20010479.
- Atallah, K., Howe, D. (1998). IEEE Trans. Magn. 34(4):2060–2062.
- Gieras, J.F., Wang, R.-J., Kamper, M.J. (2008). *Axial Flux Permanent Magnet Brushless Machines*. Springer. ISBN 978-1-4020-6993-2.
- Yazdan, T., Atiq, S., Kwon, B.-I. et al. (2019). “Two-Phase Dual-Stator Axial-Flux PM BLDC Motor With Ironless Rotor Using Only-Pull Drive Technique.” IEEE Access 7:82144–82153. DOI 10.1109/ACCESS.2019.2924011.

*Magnet material specifications and coherence:*

- Arnold Magnetic Technologies. Recoma 35E (Sm<sub>2</sub>Co<sub>17</sub>), N52, and N42SH datasheets. arnoldmagnetics.com.
- Gutfleisch, O. et al. (2011). “Magnetic Materials and Devices for the 21st Century.” Adv. Mater. 23:821–842. DOI 10.1002/adma.201002180.
- Coey, J.M.D. (2010). *Magnetism and Magnetic Materials*. Cambridge University Press.

*Multiplicative efficiency: quantum-thermodynamic precedents:*

- Scovil, H.E.D., Schulz-DuBois, E.O. (1959). “Three-Level Masers as Heat Engines.” Phys. Rev. Lett. 2:262.
- Scully, M.O. et al. (2011). “Quantum heat engine power can be increased by noise-induced coherence.” PNAS 108(37):15097–15100.
- Brandner, K., Bauer, M., Seifert, U. (2017). “Universal Coherence-Induced Power Losses of Quantum Heat Engines.” arXiv:1703.02464.
- Klatzow, J. et al. (2019). Phys. Rev. Lett. 122:110601.

*Motor efficiency standards and loss-model canon (additive convention):*

- IEC 60034-2-1:2024. International Electrotechnical Commission. [Rotating electrical machines — methods for determining losses and efficiency.]
- IEEE Std 112-2017. [IEEE Standard Test Procedure for Polyphase Induction Motors and Generators.]



- Fitzgerald, A.E., Kingsley, C., Umans, S.D. (2014). *Electric Machinery*, 7th ed. McGraw-Hill.
- Krause, P.C., Wasynczuk, O., Sudhoff, S.D., Pekarek, S.D. (2013). *Analysis of Electric Machinery and Drive Systems*, 3rd ed. Wiley-IEEE.

*Machine signature analysis and remainder diagnostics:*

- Thomson, W.T., Fenger, M. (2001). IEEE Ind. Appl. Mag. 7(4):26–34. DOI 10.1109/2943.930988.
- Kliman, G.B. et al. (1988). IEEE Trans. Energy Convers. 3(4):873–879. DOI 10.1109/60.9364.
- Randall, R.B., Antoni, J. (2011). Mech. Syst. Signal Process. 25(2):485–520. DOI 10.1016/j.ymssp.2010.07.017.
- Cavina, N., Corti, E., Minelli, G., Serra, G. (2002). SAE Technical Paper 2002-01-0480. DOI 10.4271/2002-01-0480. [Four-stroke IC engine  $\omega/2$  misfire diagnostics — nearest prior art for half-order content as designed operating line.]

*License and trademark notice*<sup>1</sup>

---

<sup>1</sup>© 2026 Resonant Institute. This work is licensed under the Creative Commons Attribution-NonCommercial-ShareAlike 4.0 International License (CC BY-NC-SA 4.0). *Energetic First Principles* and *E1P* are trademarks of Resonant Institute.